Contents lists available at ScienceDirect

Journal of Energy Storage

journal homepage: www.elsevier.com

Journal Cover Image

Lithium-ion capacitor safety assessment under electrical abuse tests based on ultrasound characterization and cell opening

L. Oca [a, b, *], N. Guillet [a], R. Tessard [a], U. Iraola [b]

[a] Univ. Grenoble Alpes, CEA, LITEN, DTS, INES, F-38000 Grenoble, France
[b] Mondragon Unibertsitatea, Electronic and Computing Department, 4 Loramendi, Mondragon, 20500, Basque Country, Spain

ARTICLE INFO

Keywords:
Lithium-ion capacitor
Over-charge
Under-discharge
Safety
Ultrasound characterization

ABSTRACT

Safety issues related to lithium-ion batteries are a driving force in the search for new energy storage systems. Lithium-ion capacitors are becoming recognised as promising devices to address the question of safety. These products are a combination of lithium-ion batteries and electric double-layer capacitors in terms of energy and power density. The aim of this work is to assess lithium-ion capacitor safety under over-charge and under-discharge processes for pouch and prismatic cells. In the course of performing abuse tests, no evidence was found of severe hazard (explosion, fire or flame, rupture or major leakage). Quantitative external parameters (thickness, resistance and mass) and electro-thermal measurements showed an increase of swelling and internal resistance, which caused a decrease of capacity and energy efficiency in all cases. The ultrasound characterization technique confirmed that there were irreversible physical modifications of the materials under abuse conditions on prismatic cells, which could not be seen with the commonly used magnitudes (U, I, T). This technique was also used for the identification of the start of cell degradation. In post-mortem analysis, were observed different degradation phenomena such as melting of the separator and delamination in the electrodes.

1. Introduction

The world is undergoing an energetic revolution moving from the unsustainable fossil-fuel based energy approach to renewable energies. Added to that, some forecasts show a trend of increasing demand on world energy consumption over the next three decades due to the industrialization of non-developed countries. In 2040, the annual world energy consumption is expected to reach more than 200.10^{12} TWh [1]. Therefore, we must reform the generation, transmission, distribution and storage of energy to cope with future needs [2,3].

Energy Storage Systems must evolve and adapt, as they are a key factor in applications such as renewable energies, smart grids, transport and consumer electronics. Renewable energies, the use of which is on the rise, rely heavily on energy storage systems as the generation of such energy is random and heavily dependent on climatic conditions [4]. Its distributed generation causes a reform on the distribution of energy, tending to smart grids [5]. Moreover, electro-mobility applications (trains, trams, electric vehicles etc.) are a critical research area as it is highly dependent on the advances of new storage systems [6]. In the past few years, the number of electronic devices such as laptops and mobile phones has increased while batteries are developed [7]. That is why we need to upgrade cells to improve safety, durability and performance (power density, energy density, efficiency in a wide temperature range) with a decrease of the cost.

One of the most critical issues for energy storage systems is safety. Nowadays, Lithium Ion Batteries (LIBs) are dominant in applications such as consumer electronics or transportation due to their high energy density [8]. However, the tight operational safety window, the lack of power density, their limited cycle life and cost are the major drawbacks of this technology [9,10]. Safety in lithium-ion batteries is probably, the main factor that causes the lack of confidence in this technology, as we must guarantee human safety in all applications. Recently, some incidents with LIBs resulting in fires or explosions in electric vehicles [11], laptops, mobile phones or electronic cigarettes [12] have drawn considerable attention [13]. This raises the question of whether lithium-ion batteries are ready and safe enough for everyday use. Conventional Electric Double-Layer Capacitors (EDLCs) are safe devices, however their low energy density means that they are usually used as high-power buffers in conjunction with batteries [14].

* Corresponding author at: Univ. Grenoble Alpes, CEA, LITEN, DTS, INES, F-38000 Grenoble, France.
Email address: lauraoca@mondragon.edu (L. Oca)

https://doi.org/10.1016/j.est.2019.02.033
Received 11 January 2019; Received in revised form 28 February 2019; Accepted 28 February 2019
Available online xxx
2352-152/

In order to surpass the main shortcomings of electrochemical storage systems, new materials and configurations are being widely studied [15,16]. Among them, lithium-ion capacitors (LiCs) are a promising energy storage technology, which combines a supercapacitor-like electrode (non-faradaic electrode) with a battery-like electrode (faradaic electrode). On the one hand, activated carbon is used for the positive electrode where a rapid lithium ion adsorption-desorption process occurs on the surface area [17]. On the other hand, the negative electrode is mainly composed of graphite or hard carbon materials in which a lithium insertion/deinsertion process predominates. In opposite to LIBs, LiCs require a pre-lithiation process of the negative electrode. Different strategies can be used for the pre-lithiation of the negative electrode, depending on the source of lithium ions: sacrificial metallic lithium electrode, dissolved lithium salt contained in the electrolyte or over-lithiated transition metal oxides in the positive electrode [18]. Moreover, recent studies shows different material combinations to increase the performance of those devices [19]. LiC devices are more efficient, have faster charge-discharge cycles, are safer and can provide higher current density than LIBs. In contrast to EDLCs, LiCs have higher energy density (more energy per unit of mass) and a more useful operational voltage range for applications (3.8 V to 2.2 V in LiCs vs 2.7 V to 0 V in EDLCs) [20]. Hence, external circuits that augment complexity of the system are reduced.

In order to launch new products in the market, it is important to assess the safety of the technology. Researchers use widespread abusive tests such as nail penetration, short circuit, over-charge, under-discharge and thermal stability to evaluate safety. Different standards are available in the literature for LIBs and EDLCs [21], however, to our knowledge; no common method has been established for LiCs. It is necessary to identify the causes that could lead to abnormal operation of the cells. For example, a malfunction of the charger or inappropriate design of the battery management system (BMS) could cause an over-charge (OC) or under-discharge (UD) of the devices. Furthermore, improper use could cause cells to reach a very low voltage, resulting in cell failure (up to 0 V). The over-charge and under-discharge processes of an LIB have been investigated in depth in the literature [22,23]. In a deep under-discharge of an LIB, the metal-oxide based material of the positive electrode host structure is destroyed due to the over-lithiation process. The release of oxygen could cause the decomposition of organic electrolyte and increase the inner temperature of the cell. Under these conditions, the entire cell becomes unstable leading to a thermal runaway [23].

To overcome this, BMSs are used to ensure that cells work within the safe operating window, preventing different kinds of events [24], which are defined by the EUCAR hazard table [25]. In a BMS, voltage, current and temperature magnitudes are monitored. Despite the fact that those three magnitudes are commonly used, very little is known about the internal stability of the cells after abuse tests [26]. It is possible to employ techniques such as ultrasound characterization to analyse and identify physical changes in the cell materials during ageing and cycling. Ultrasound characterization (UsC) is an active non-destructive technique of characterization in which acoustic waves of a defined wavelength are injected from a piezoelectric transducer within the sample material. The acoustic waves interact with the materials and can be absorbed or reflected by defects [27]. It provides real time information about physical changes in the materials, structural evolution *operando*, state of charge (SoC) and state of health of the cells to identify future failures or abnormal behaviour [26–29].

Post-mortem analysis provides an overview of the inner damage of the cells after the abuse tests. The opening of the cell gives more information about the inner degradation of the cells in a specific state. In the literature, many studies have been undertaken to determine the failure mechanisms and degradation phenomena in LIBs [30].

To our knowledge, exhaustive analysis of lithium-ion capacitors during over-charge and under-discharge processes have not been done. There are some qualitative results of JM Energy products evaluated by NASA in collaboration with JSR Micro Inc. [31] in which the researchers affirm that LiCs did not show venting or fire during the OC and UD tests [32]. However, the study of degradation phenomena or stability of the cells after abuse tests where not in scope of that project.

The aim of this work is to study the over-charge and under-discharge processes of lithium-ion capacitors giving quantitative results and insight view of the material changes of the cell with two different forms (pouch and prismatic cells). In the study, several topics are covered: evaluation of external parameters of the cells (thickness, resistance and mass), monitorization of electro-thermal magnitudes, physical modification analysis via ultrasound characterization technique and post-mortem analysis.

2. Experimental set-up: cells, equipment and procedure

2.1. Main characteristics of the cells and test equipment

In this paper, two commercial lithium-ion capacitor products are investigated and compared: 1100 F pouch and 3300 F prismatic cells manufactured by JM Energy [33]. The electrical specifications of the cells are shown in Table 1. For both cells, the active material of the negative electrode is made of graphite, while the positive electrode is made of activated carbon. The electrolyte is a mixture of lithium hexafluorophospate salt ($LiPF_6$) with commonly used organic solvents (ethyl methyl carbonate, ethylene carbonate and dimethyl carbonate).

To ensure the safety of the experiment, the tests were performed under controlled conditions inside a THT EV + Accelerating Rate Calorimeter. A BCS815 BioLogic cycler was used for cell cycling and recording the external temperature of the cell. To measure the resistance at 1 kHz, a Hioki BT3554 battery tester was employed. Moreover, the mass was measured with a precision balance with ± 1 g of maximum error.

During the abuse test of the prismatic cells, the UsC was employed as an *operando* monitoring technique. The acoustic emission (AE) equipment is composed of several components: piezoelectric transducers, an amplifier, pass band filters and a data acquisition/digital signal processing system (PCI-2 AE, multi-channel board & system, Physical Acoustic Corporation, MISTRAS Group, Inc.). The AE signals were visualized and recorded by the software AEWIN for PCI2 (Physical Acoustic, MISTRAS Group, Inc.). Ultrasound characterization setup is composed of two small ceramic piezoelectric transducers EPZ-27MS44 W. The first one is excited by an electric signal with frequency sweeping between 120–500 kHz (200 ms) generated by an ARB-1410 Arbitrary Waveform Generator Board designed on the WaveGen1410 Software (Physical Acoustic Corporation, MISTRAS Group, Inc.). The vibration generated by the first transducer is transmitted throughout the battery and detected by the second transducer. This vibration is converted into an electrical signal and recorded with the same measuring chain as for AE signals.

After the abuse test of the pouch cells, they were opened in an Argon environment, in a Jacomex glovebox, to determine the possible causes of failure.

Table 1
Main characteristics of analysed products [29].

Characteristics	1100 F LiC	3300 F LiC
Range of operating temperatures (ºC)	−30 – 70	−30 – 70
Operating voltage range (V)	2.2 – 3.8	2.2 – 3.8
Capacitance (F)	1100	3300
Capacity (Ah)	0.5	1.5
ESR (mΩ)	0.8	0.7
Energy Density (Wh kg^{-1})	10	13
Mass (kg)	0.144	0.350

2.2. Over-charge and under-discharge test procedure

In order to define a test protocol for LiCs, data available of LiC abuse tests in the literature was collected. JM Energy provide information about test conditions and general results of the OC and UD abuse tests [31,32]. They performed tests in two different ways, and no quantitative results were given (see Table 2).

In this research, for the over-charge of the pouch cell, the applied charge current was 5 A, which corresponds to a rate of 10C of the cell and the test limit was set to twice the maximum voltage of the cell (7.6 V). Additionally, a capacity limit of 200% was established in order to compare results, however the abuse test was continued until the cell was completely damaged. For the under-discharge of the pouch cell, the same current was applied (5 A) to be able to compare the results, and the voltage limit was set to 0 V. This procedure enables comparing external and electro-thermal measurements (U, I, T) of both tests and assessing the degradation phenomena after opening the cells. In both cells, the test started from the storage voltage of 3 V.

For the prismatic cell, a different test procedure was followed. Firstly, three normal cycles at 10 A (6.6C) and operating voltage range (3.8 V – 2.2 V) were performed. This allowed us to record the acoustic signal in the normal operating conditions that serves as a reference for the abuse tests. Then, two mild-charge/discharge cycles up to 4.5 V and 2.0 V were done. Those cycles determine if cells remain stable (under these conditions) or present an abnormal behaviour. Finally, 5 A (3.3C) of constant current charge/discharge was set for the full over-charge or under-discharge. As in the case of the pouch cell, 200% of rated capacity was set as a comparable limit, although the test continued until the complete damage or 7.6 V.

3. Results and discussion

In this work, over-charge and under-discharge tests were evaluated addressing several topics: (1) quantification of the variation of external parameters (thickness, resistance and mass); (2) abnormal behavior identification based on electro-thermal parameters (U, I, T); (3) stability of the cells and irreversible physical modifications of materials with UsC; and (4) degradation phenomena of lithium-ion capacitors after abuse tests.

Table 2
Test conditions and general results for LiCs from sources [31,32]. NI: no information.

Tests	Conditions	Fire	Rupture	Explosion
Over-charge [29]	Current: 200 A SoC: 250 % Max voltage: 20 V with constraining unit	Not observed	Not observed	NI
Over-charge [30]	Charge up to 250 % of rated capacitance with 1 A constant current	Pass	NI	Pass
Under-discharge [29]	Current: 200 A Voltage: 0 V	Not observed	Not observed	NI
Under-discharge [30]	Discharge to 0 V with 1 A constant current	Pass	NI	Pass

3.1. Visual inspection and external parameters

In order to quantify the swelling rate, cells thickness was measured in the centre of the cell (where higher difference is expected) (see Table 3). It is difficult to quantify the maximum variation of the thickness, as after the abuse test several cycles on the operational voltage range were performed to analyse the remaining capacity and resistance of the cell. The thickness after abuse test was measured for all cases in a discharged state. All the cells were significantly swollen after the abuse tests. Unsurprisingly, the swelling rate of the pouch cells was far more important than for the prismatic cell, for both the OC and UD tests. Furthermore, the OC test showed higher swelling rate, which could mean that the over-charge process is more harmful to these devices and probably leads to higher gas evolution. A similar tendency was observed in the resistance (Table 3). In all the cases, the resistance increased, but a lower increase occurred in under-discharge. For the prismatic cell, this was negligible. No significant difference was observed in the under-discharged cells; the small variation of mass measured before and after the tests was due to balance imprecisions (Table 3). However a 6.2% and 3.3% decrease were measured in over-charged pouch and prismatic cells, respectively.

A visual inspection of the over-charged pouch cell revealed that the gas made a path on the left side of the safety valve (when the positive tab was on the left side). A small amount of electrolyte was stored between the metallic case and a thin plastic film covering the case, which indicates that a small leak occurred (Fig. 1a). As for the over-charged prismatic cell, the safety valve was opened, causing a slight mass loss (Fig. 1b). On the other hand, for the under-discharged cells (both configurations), visual inspection did not find evidence of any venting (Fig. 1c, d).

From the visual inspection and external measurements, it was possible to conclude that there was no severe hazard such as explosion, fire or flame, rupture and major leakage. A minor leakage in the over-charged products was reported. Considerable swelling was noted in the under-discharged pouch cells, so, irreversible damage makes replacement or repair needed. For the prismatic under-discharged cell, no significant signs of degradation were reported based on those results. Fig. 1 shows the final shape of the four samples tested.

3.2. Electro-thermal parameter evaluation

For both LiCs cells, during normal cycling (2.2–3.8 V) at room temperature and low current, the cell temperature slightly decreases during charge and increases during discharge. This is the sign that endothermal processes occur during charge, and that the energy absorbed from the surrounding is only partially compensated by the Joule effect (RI^2).

The heat transferred reversibly to the surrounding (Q_{rev}) was measured by heat flux sensors on the prismatic LiC cells in a thermal chamber set at 25 °C during cycling at a constant current of 5 A (see Table 4). It was found to be 1032 J (189 mJ/C). The heat exchanged with the

Table 3
Initial and final external parameter comparison. *1Internal resistance and mass were measured for the over-charged cells when the cell was completely damaged, not when the cell reached twice capacity.

Cell	Test	Thickness (mm)			Resistance (mΩ)*1			Mass (g)*1		
		Initial	Final	Swelling rate (%)	Initial	Final	Difference (%)	Initial	Final	Difference (%)
LiC pouch	OC	5.3	53.0	900	0.8	234.0	27592	145	136	−6.2
LiC pouch	UD	5.5	37.8	587	0.9	2.19	158	145	144	−0.7
LiC prism	OC	15.7	26.2	67	0.7	1.3	74	360	348	−3.3
LiC prism	UD	16.0	16.5	3	0.8	0.8	0	358	360	0.5

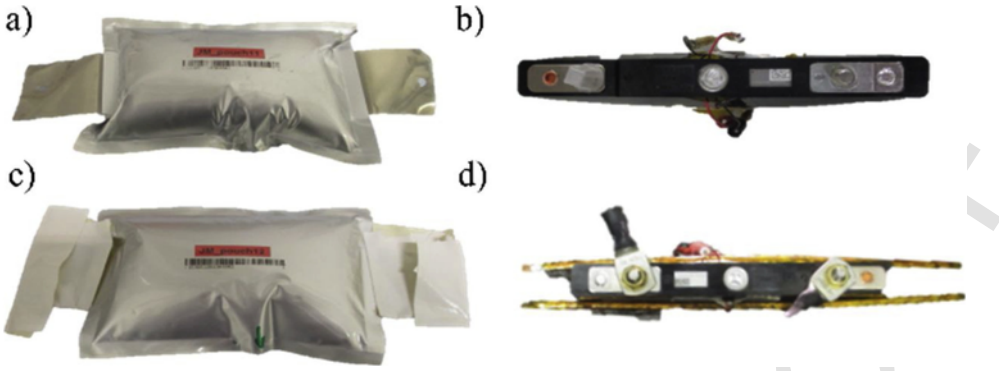

Fig. 1. Visual inspection of tested cells after the abuse tests. a) 1100 F pouch OC; b) 3300 F prism OC; c) 1100 F pouch UD; d) 3300 F prism UD.

Table 4
Electro-thermal parameters of prismatic and pouch cells calculated from heat flux sensors measurements during charge - discharge cycling at a continuous current of 5 A.

		Q_{tot} (J)	Q_{rev} (J)	Q_{irrev} (J)	$\int_{t_0}^{t_1} i(t)^2 dt$ (A^2.s)	$R_{equivalent}$ (mΩ)
Prismatic cell 1.5 Ah	Charge	−917	−1,032	115.7	27,050	4.24
	Discharge	1,147	1,032	115.5	27,240	
Pouch cell 0.5 Ah	Charge	−199	−235	36.5	9,011	4.05
	Discharge	272	235	36.9	9,111	

surrounding was negative during charge and positive during discharge. At the same time, the total heat lost to the surroundings (Q_{irrev}) by Joule effect during both charge and discharge only reaches 115 J (internal equivalent resistance of 4.2 mΩ). During charge at 5 A, the energy exchanged with the surrounding is thus clearly negative with −917 J (decreases the cell temperature) and positive during discharge with 1147 J (increases the cell temperature).

Pouch cell tests (OC and UD) started at 3.0 V. During the normal charge, up to 3.8 V, the endothermic process took place in the cell as the cell temperature remained stable or even slightly decreased (see Fig. 2a). When the cell voltage exceeded 3.8 V (normal cut-off voltage), the cell showed an exothermic reaction. At first, the temperature rose slightly and then increased sharply when the charge exceeded 150% of the nominal capacity. This is probably mainly due to exothermic oxidation reaction of the electrolyte, resulting in the production of gaseous products at both positive [34–37] (CO_2) and negative electrodes [37,38] (CO, C_2H_4…), and the swelling of the cell.

During under-discharge test of the pouch cell, the voltage decreased almost linearly until 0.5 V (see Fig. 2a) while the temperature of the cell increased sharply. At that stage, the potential of the graphitic electrode is expected to increase and the copper foil used as the negative electrode current collector can start to oxidize to copper ions. A different behavior occurs in the voltage range of 0.5 V – 0 V which is not appreciable in the prismatic cell. Just before reaching 400% of discharge, the temperature of the cell decreased. This could be due to the swelling of the cell. After the full discharge, the relaxation of the voltage was measured, rising to 0.33 V; thus, the 0 V state was not at equilibrium.

Similar voltage and temperature evolution with charge were noted for the pouch and prismatic cells. For the prismatic cells, the endothermic process occurred in the charge process up to 150% of the nominal capacity, at voltages lower than 4.4 V (see Fig. 2b). Then, the temperature of the cell increased and the cell voltage reached the maximum value of 5.0 V at 200% of the nominal capacity. The over-charge period was continued (not plotted in Fig. 2b), the voltage dropped gradually while the cell temperature increased until 76 °C (which exceeded the maximum temperature limit of the cells of 70 °C). In the region of the maximum temperature, the vent opened, and the temperature started to decrease. During under-discharge, the behaviour of prismatic cell was very close to the one reported for pouch cell.

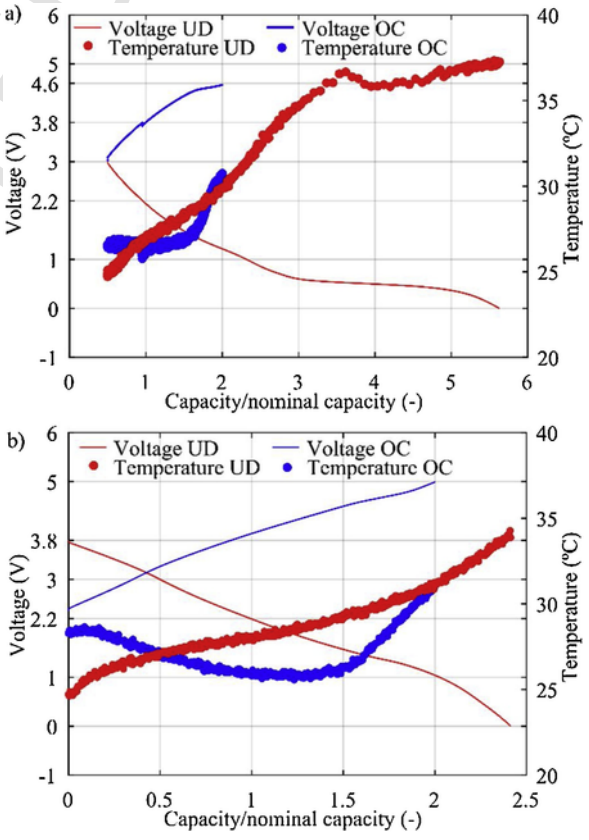

Fig. 2. Voltage and temperature evolution during abuse tests. a) OC/UD of pouch cells; b) OC/UD of prismatic cells.

In Table 5, the main results of electro-thermal parameters for the abuse tests are summarized. The energy density during the OC is higher than for the UD, as the voltage range used during the abuse test was wider. The under-discharge process of the pouch cell presented an unexpected behaviour that is reflected in the obtained value for the capacity. For all the cases, the coulombic and energy efficiency of the

Table 5
Electro-thermal parameter comparison. *1Data from 2.2 V to 3.0 V were calculated based on previous normal cycles of the same cell, in order to obtain comparable results with the prismatic cell. Capacity obtained directly from the experiment appears between brackets which corresponds to the abuse test starting from 3.0 V. *2For the over-charged cell, the cell was discharged to remove the remaining energy until a voltage of 2.2 V. For the under-discharged cell, no evaluation cycles were performed at the end of the abuse tests, as the aim was to open the cell at the complete under-discharged state.

Characteristics		OC pouch	UD pouch	OC prismatic	UD prismatic
Voltage (V)	Initial	3.0	3.0	2.2	3.8
	Final	4.6	0.0	5.0	0.0
Temperature (ºC)	Initial	26.6	24.8	28.3	24.7
	Maximum	30.7	37.3	31.1	33.9
Capacity per mass (Ah kg^{-1})	Normal cycle	3.5	3.5	4.0	4.0
	Abuse test	6.9 (5.6)*1	19.4 (18.1)*1	8.6	6.9
	Faradaic efficiency after test (%)	86.6*2	-*2	90.6	96.2
Energy density (Wh kg^{-1})	Normal cycle	10.4	10.4	11.7	11.7
	Abuse test	26.4 (20.8)*1	22.2 (16.7)*1	33.1	20.6
	Energy efficiency after test (%)	22.3*2	-*2	75.0	84.2

cells in the last cycles decreased, which indicates that there is evidence of parasitic reactions after the abuse test.

Taking into account the electrical parameter control and the external temperature of the cell, we cannot confirm that the cell was not damaged after a short period of OC or UD. With a small increase or decrease of the voltage out of the normal operating range, it was not possible to see significant modifications of the voltage path or temperature profile. To overcome to that problem, the acoustic emission technique was employed for prismatic cells, to evaluate the techniques for advanced device monitoring.

3.3. Ultrasound characterization during abuse tests

Ultrasound characterization allows early detection of signs of degradation in abnormal operating conditions (over-charge, under-discharge). Indeed, each cell has conservative fixed operation limits, set by the manufacturer. However, it is possible to limit premature loss of cell performance by adapting the operation conditions (voltage and current). Accurate device monitoring enables the collection of *operando* information from the cell behaviour. In this section, two conditions outside the safe voltage window are analysed and discussed: higher voltage than the manufacturer operating region (mild over-charges up to 4.5 V and full over-charge) and lower voltage of the operating region (mild under-discharge up to 2.0 V and full under-discharge).

To compare the evolution during abuse tests, reference cycles were performed under normal conditions (Fig. 3a). In the Fig. 3b, the evolution of the acoustic signal strength [39] transmitted through the cell during the experiment (one normal cycle 2.2–3.8 V, followed by two cycles with mild over-charge 2.2–4.5 V, then full over-charge 2.2–5.2 V) is shown.

Each acoustic signal recorded is reported on the voltage versus time and signal strength versus time diagrams as coloured dots. The colour is attributed after applying a clustering method of analysis based on the Euclidean distance between each signal recorded. A 2D representation map based on the nearest neighbour classifier is used and each point refers to a registered waveform. The X and Y axis do not have any physical signification (the map is invariant by rotation and symmetry). Thereafter, the proximity between waveforms is coded by colour of points. A specific colour is attributed to each waveform, as a function of its position on the map. Points with similar colour correspond to similar acoustic signal waveforms.

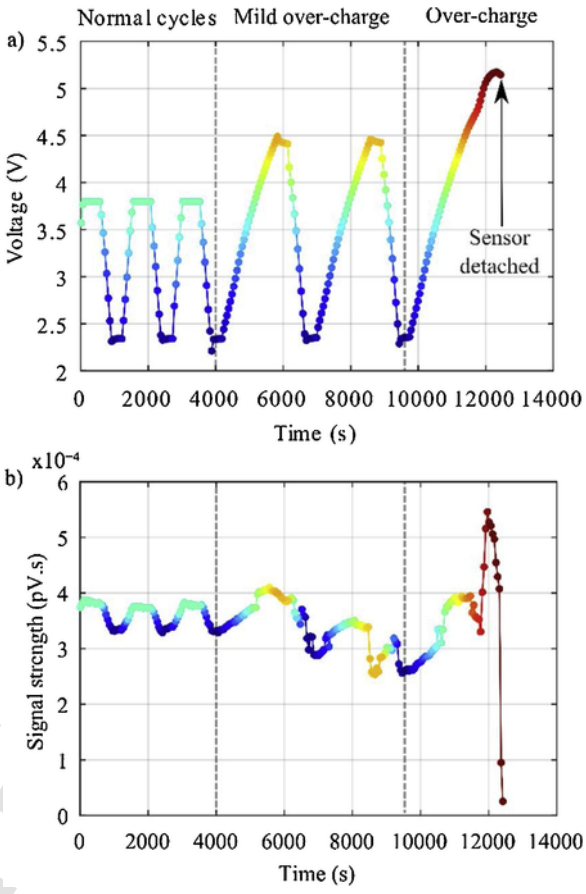

Fig. 3. Acoustic signal in OC a) Voltage vs time plot; b) Signal strength vs time plot.

During the normal charge – discharge cycle (2.2–3.8 V), the colour of the dots changed from light blue (fully discharged state, signal strength of 33 nV.s) to green (fully charged state, signal strength of 40 nV.s), which would indicate that UsC measurements are repeatable. The measurements are highly sensitive to very small differences in waveforms. Moreover, the mapping for normal cycles of the prismatic cell shown in Fig. 4.a, presents a repeated path of points going from discharge to charge state.

3.3.1. Mild and full over-charge characterization

Two mild over-charge cycles are shown in Fig. 3, after the last cycle under normal operating conditions. The same colors were seen until 3.8 V (upper voltage limit in normal range). However, at the end of the first over-charge (6000 s) abnormal behavior clearly appeared on the acoustic signal (Fig. 3b). Whereas the electrical signal appeared normal, acoustic signal revealed that the system became unstable. The signal strength started to decrease and did not follow the pattern of previous cycles. During the complete over-charge, the signal strength was higher than previous cycles, as shown in Fig. 3b. We obtained the greatest change of the acoustic signal during the full over-charge (between 4.5 V and 5.2 V). After 5.2 V, the piezoelectric sensor lost contact with the casing of the cell, due to the swelling of the cell. Therefore, no more signals were recorded.

In Fig. 4b, it is possible to see the mapping during the entire over-charge test. Several clusters of points can be identified, which are highlighted in circles with different colors. The first mild over-charge up to 4.5 V is similar to that presented in Fig. 4a for normal cycles. However,

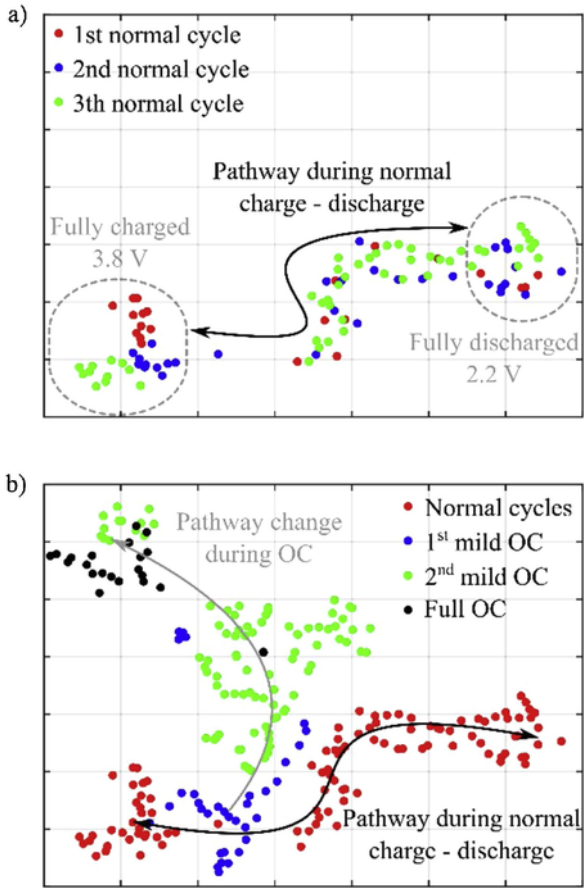

Fig. 4. Mapping for OC of prismatic cell. a) Normal cycling; b) All the cycles.

a significant change during the next discharge was observed and the evolution continued during the second mild over-charge. After the full over-charge, the completely discharged state was completely different to previous cycles.

The time of flight (ToF) of the over-charge test was also analysed. The ToF represents the duration between the signal emission and the signal reception. The greater the ToF, the greater the distance between the emitter and receptor. This suggests a relationship between swelling and the ToF (see Fig. 5a). In the over-charge of the prismatic cell, the ToF increased after the first mild-OC, during discharge. The ToF continue to rise during the next cycles (see Fig. 5b). It is interesting to note that the swelling of the cell was most likely initiated during the discharge after the first mild over-charge (de-lithiation of the graphite) and continued during the cycling thereafter. This swelling was most probably due to the gas evolution in the cell.

In conclusion, after the first mild over-charge at 4.5 V, the cell is no longer stable, as the acoustic signal is not repeatable during cycling. This was of considerable interest as we know that it is not possible to detect any difference in the electro-thermal measurements during the mild over-charge cycles. This means that those magnitudes are not sufficient to identify the abnormal behavior of the cell in that case. After full over-charge, the capacity and energy efficiency of the cells decreased as shown in Table 5, which is an indicator of malfunctioning. A rise in temperature was also reported in such tests.

3.3.2. *Mild and full under-discharge characterization*

When the lower cell voltage exceeded the minimum recommended voltage of the supplier to 2.0 V (mild under-discharge) (Fig. 6a), blue dots and lower signal strength appeared (Fig. 6b). Nevertheless after the first partial discharge, the acoustic signal of the next cycle was comparable with previous cycles. Therefore, it is possible to confirm

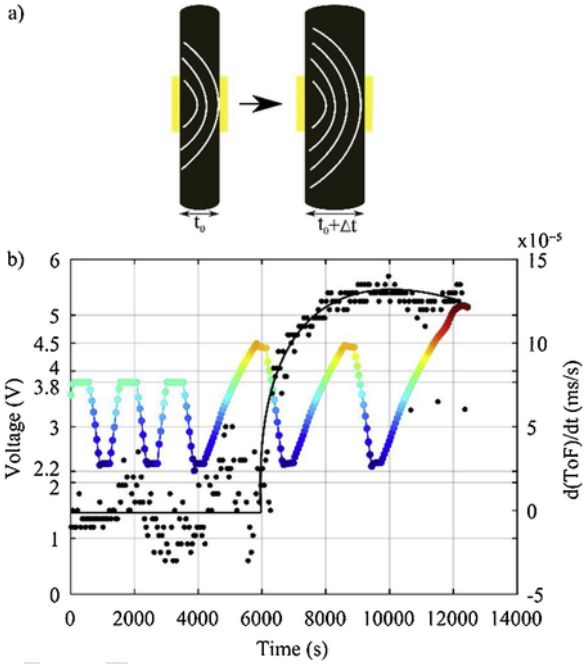

Fig. 5. Time of flight (ToF) a) ToF diagram; b) d(ToF) vs voltage and time.

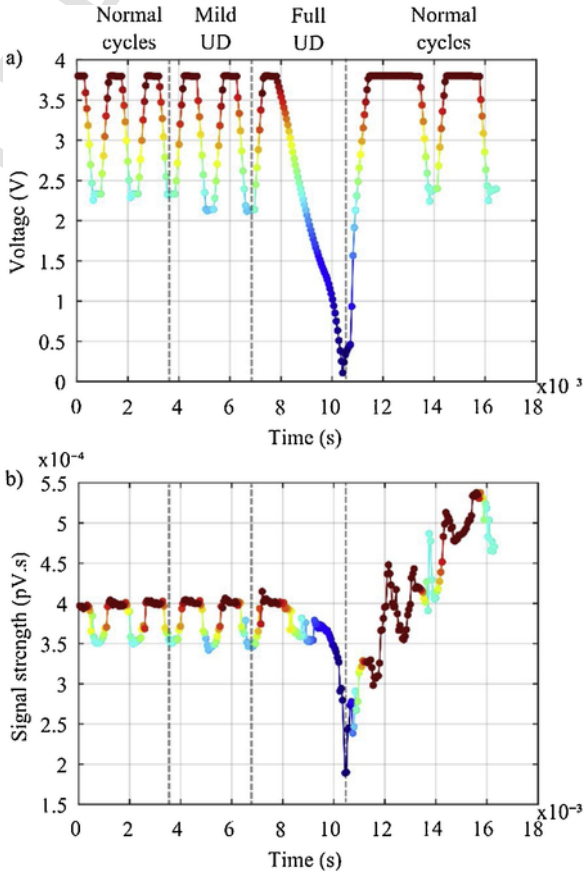

Fig. 6. Acoustic signal in UD a) Voltage vs time plot; b) Signal strength vs time plot.

that acoustic signals can be used to detect internal consequences of mild under-discharge (2.0 V). Under tested conditions, it was observed that after under-discharge at 2.0 V the cell remained stable.

The greatest change in the acoustic signal was seen in the complete under-discharge (see Fig. 6b). During the cycles after the UD, no re-

peatable pathway was observed, which suggests that the cell was unstable. Indeed, higher signal strength was recorded during the last cycles (>50 nV.s compared to 40 nV.s). Afterwards, even though it was still possible to cycle the cells, the acoustic signal was not repeatable during cycling and the coulombic efficiency of the cell decreased (sign of parasitic reactions occurring).

uring the charge process after a normal cycle (2.2 V cut-off-voltage) and mild under-discharge (2.0 V cut-off-voltage) different pathways were observed (see Fig. 7a, b). The same pathways can be seen during the constant current discharge process (except at the end of the dis-

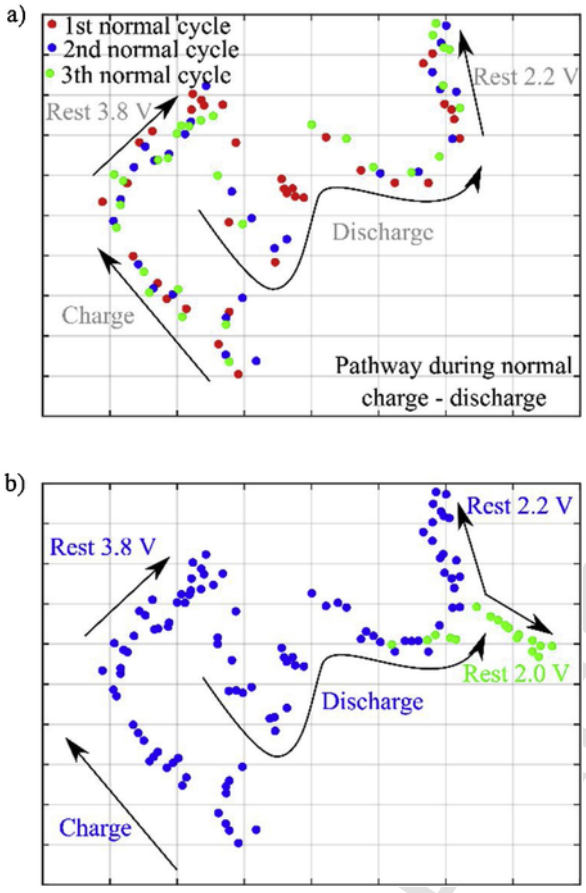

Fig. 7. Mapping for UD of prismatic cell. a) Normal cycling; b) All the cycles.

charge, SoC 0%) despite the different behaviour in the charge. There are significant differences between acoustic signals recorded at SoC 0% when the cell is discharged at 2.2 V and 2.0 V. At the end of the charge, constant voltage phase and five minutes rest period were applied, while after the discharge, only a rest period of five minutes was applied.

After mild under-discharge until 2.0 V, the cell showed all indications of remaining stable and thus could be used normally. However, after the full under-discharge, signs of irreversible damage were evident even though it could still be cycled. When the cell reached 0 V, it was immediately charged up to normal operating conditions as a long period at 0 V could also affect the degradation.

3.4. Degradation phenomena of lithium-ion capacitors

We performed a post-mortem analysis after OC and UD of pouch cells. Devices were disassembled to investigate the inner change of the components separately, and possible failure methods. For the under-discharged cell, once the case was punched and all the gas was released, no appreciable degradation of the inner cell was discerned. The appearance of some bubbles in the separator was the only sign of degradation. In contrast, the over-charged cell presented significant damage in all the components. The internal components of the over-charged cell appears in Fig. 8.

The yellow color in the first layer of separator is noticeable, which is a sign of electrolyte degradation [40]. We found that the connections of the copper current collector were more damaged than the aluminum current collector. Probably due to the oxidation of Cu to Cu^{+} (around 3.92 V vs Li/Li^{+}) and further oxidation of Cu^{+} to Cu^{2+} (around 4.17 V vs Li/Li^{+}) on the positive electrode [41]. The separator was melted in some small areas; the melted area is highlighted inside a red circle (see Fig. 8b). This indicates that a micro short circuit could have occurred inside the cell. This might be due to the dendrite growth during the lithium deposition [42]. Moreover, adhesion of the graphite electrode to the separator and gas bubbles were also seen. This suggests that the active material of the negative electrode was seriously damaged, and the gas evolution was another reason for the malfunction of the device.

The electrode degradation was more obvious in the graphitic electrode (see Fig. 8c). First, in the electrodes different colors appeared, possibly indicating that there were different SoCs in the same electrode. During the charge, lithium is inserted in the graphite. When the electrode is completely lithiated, it has a bright gold color, while it tends to darken in a non-lithiated state [28]. When the negative electrode is full of intercalated lithium LiC_6, metallic lithium is deposited and dendrites can form on the surface of the electrode. This lithium

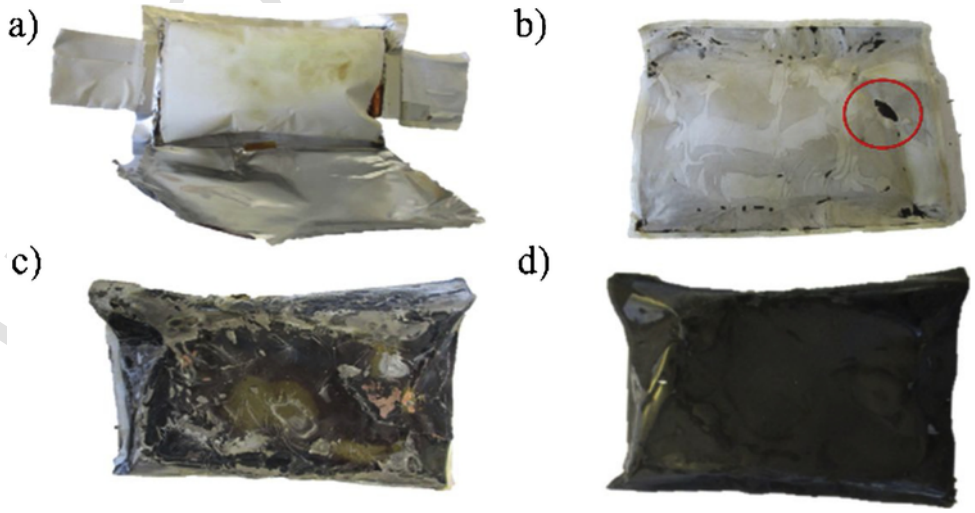

Fig. 8. Pouch cell inner components after the OC test. a) Cell; b) Separator; c) Graphite electrode; d) Activated carbon electrode.

can react with the electrolyte, increasing the Solid-Electrolyte Interphase (SEI) film, and therefore increasing the ohmic resistance of the cell [42]. The metallic lithium reacts with the solvent of the electrolyte to form Li salts. When these salts are exposed to the air the color changes to white. In the tested sample, this was evident from the white color of the degraded cell [42]. The cell was opened in a pure argon environment; however, some O_2 or H_2O ppm could also have provoked the color change. The positive electrode (activated carbon) is less degraded than the graphite electrode (Fig. 8d), although it was rigid and deformed at the time of the opening.

4. Conclusions

The purpose of the current study was to assess lithium-ion capacitor safety under electrical abuse tests. JM Energy pouch and prismatic cells were tested and the results show that are safe under tested conditions. No severe hazardous consequences like firing or explosion were reported after electrical abuse tests. In both products (pouch and prismatic LiC) the over-charge case was more harmful for the cells, in which only slight venting was observed. Due to degradation phenomena inside the cell, gas evolution increased the internal pressure causing swelling and higher internal resistance (up to 234 mΩ). In the worst case, after the over-charge process of the pouch cell, 86.6% and 22.3% of faradaic and energy efficiency were reported respectively, which is an indicator of the abnormal behaviour of the cells. After the partial OC and UD cycles, early signs of degradation were not identified with the commonly used magnitudes (U, I, T).

Under the operating range of the manufacturer (2.2–3.8 V), the signal strength of UsC measurements was repeatable, changing from a value of 40 nV.s in the charged state to 33 nV.s in the discharged state. Ultrasound characterization confirmed that there are irreversible physical modifications of the materials under abuse conditions, in both OC and UD, as the signal strength after abuse tests is higher (approximately 55 nV.s). After the mild-UD at 2.0 V the cell remained stable, whereas at 4.5 V irreversible changes in the materials occurred. Moreover, the time of flight (ToF) is a good indicator of the swelling of the cell, which was initiated during the discharge after the first mild-OC and increased linearly during cycling thereafter. Via the post-mortem analysis different degradation phenomena were directly seen, such as melting of the separator and adhesion loss of the graphitic electrode.

Acknowledgements

The authors would like to thank Mr. S. Dumenil for the provided help during the tests, Mr. J. M. Klein for the kindly support during the research and Mr E. Miguel for the valuable advices on writing the paper.

References

[1] U.S. Energy Information Administration (EIA), International Energy Outlook, in: https://www.eia.gov/outlooks/ieo/pdf/0484(2017).pdf, 2017, (Accessed 09 January 2019).
[2] N. Edomah, C. Foulds, A. Jones, Influences on energy supply infrastructure: a comparison of different theoretical perspectives, Renew. Sustain. Energy Rev. 79 (2017) 765–778, https://doi.org/10.1016/j.rser.2017.05.072.
[3] World Economic Forum, Global Energy Architecture Performance Index Report 2017, 2017, Genevahttps://www.weforum.org/reports/global-energy-architecture-performance-index-report-2017(Accessed 09 January 2019).
[4] L. Fara, D. Craciunescu, Output analysis of stand-alone PV systems: modeling, simulation and control, Energy Procedia 112 (2017) 595–605, https://doi.org/10.1016/j.egypro.2017.03.1125.
[5] S. Daiva, G. Saulius, A. Liudmila, Energy distribution planning models taxonomy and methods of distributed generation systems, Energy Procedia 107 (2017) 275–283, https://doi.org/10.1016/j.egypro.2016.12.150.
[6] H. Auvinen, T. Järvi, M. Kloetzke, U. Kugler, J.-A. Bühne, F. Heinl, J. Kurte, K. Esser, Electromobility scenarios: research findings to inform policy, Transp. Res. Procedia 14 (2016) 2564–2573, https://doi.org/10.1016/j.trpro.2016.05.346.
[7] H.F. Amjed, P. Kaliannan, Energy storage systems for energy management of renewables in distributed generation systems, in: Lucian Mihet-Popa (Ed.), Energy Management of Distributed Generation Systems, InTech, 2016, pp. 157–181, https://doi.org/10.5772/62766.
[8] J. Warner, The Handbook of Lithium-Ion Battery Pack Design: Chemistry, Components, Types and Terminology, Lithium-Ion Battery Applications, Elsevier, 2015177–209.
[9] J.-M. Tarascon, M. Armand, Issues and challenges facing rechargeable lithium batteries, Nature 414 (2001) https://doi.org/10.1038/35104644, https://doi.org/359-367.
[10] B. Scrosati, J. Garche, Lithium batteries: Status, prospects and future, J. Power Sources 195 (2010) 2419–2430, https://doi.org/10.1016/j.jpowsour.2009.11.048.
[11] X. Feng, M. Ouyang, X. Liu, L. Lu, Y. Xia, X. He, Thermal runaway mechanism of lithium ion battery for electric vehicles: a review, Energy Storage Mater. (2018) 246–267, https://doi.org/10.1016/j.ensm.2017.05.013.
[12] K.J. Nicoll, A.M. Rose, M.A.A. Khan, O. Quaba, A.G. Lowrie, Thigh burns from exploding e-cigarette lithium ion batteries: first case series, Burns 42 (2016) 42–46, https://doi.org/10.1016/j.burns.2016.03.027.
[13] Q. Wang, P. Ping, X. Zhao, G. Chu, J. Sun, C. Chen, Thermal runaway caused fire and explosion of lithium ion battery, J. Power Sources 208 (2012) 210–224, https://doi.org/10.1016/j.jpowsour.2012.02.038.
[14] G. Xiong, A. Kundu, T.S. Fisher, Thermal management in electrochemical energy storage systems, Thermal Effects in Supercapacitors, Springer Briefs in Thermal Engineering and Applied Science, 20151–10.
[15] N. Nitta, F. Wu, J. Tae Lee, G. Yushin, Li-ion battery materials: present and future, Mater. Today 18 (5) (2015) 252–264, https://doi.org/10.1016/j.mattod.2014.10.040.
[16] Y. Wang, R. Chen, T. Chen, H. Lv, G. Zhu, L. Ma, C. Wang, Z. Jin, J. Liu, Emerging non-lithium ion batteries, Energy Storage Mater. 4 (2016) 103–129, https://doi.org/10.1016/j.ensm.2016.04.001.
[17] P.H. Smith, T.N. Tran, T.L. Jiang, J. Chung, Lithium-ion capacitors: electrochemical performance and thermal behavior, J. Power Sources 243 (2013) 982–992, https://doi.org/10.1016/j.jpowsour.2013.06.012.
[18] P. Jézowski, O. Crosnier, E. Deunf, P. Poizot, F. Béguin, T. Brousse, Safe and recyclable lithium-ion capacitors using sacrificial organic lithium salt, Nat. Mater. 17 (2018) 167–173, https://doi.org/10.1038/NMAT5029.
[19] Y. Wu, F. Wang, Z. Liu, X. Yuan, J. Mo, C. Li, L. Fu, Y. Zhu, X. Wu, Quasi-solid-state Li-ion capacitor with high energy density based on Li3VO4/Carbon nanofibers and electrochemically-exfoliated graphene sheets, J. Mater. Chem. A 5 (2017) 14922–14929, https://doi.org/10.1039/C7TA03920D.
[20] J.R. Miller, Engineering electrochemical capacitor applications, J. Power Sources 326 (2016) 726–735, https://doi.org/10.1016/j.jpowsour.2016.04.020.
[21] V. Ruiz, A. Pfrang, A. Kriston, N. Omar, P. Van den Bossche, L. Boon-Brett, A review of international abuse testing standards and regulations for lithium ion batteries in electric and hybrid electric vehicles, Renew. Sustain. Energy Rev. 195 (2017) 1427–1452, https://doi.org/10.1016/j.rser.2017.05.195.
[22] H.-F. Li, J.-K. Gao, S.L. Zhang, Effect of overdischarge on swelling and recharge performance of lithium ion cells, Chin. J. Chem. 26 (2008) 1585–1588, https://doi.org/10.1002/cjoc.200890286.
[23] Q.F. Yuan, F. Zhao, W. Wang, Y. Zhao, Z. Liang, D. Yan, Overcharge failure investigation of lithium-ion batteries, Electrochim. Acta 178 (2015) 682–688, https://doi.org/10.1016/j.electacta.2015.07.147.
[24] M.A. Hannan, M.S.H. Lipu, A. Hussain, A. Mohamed, A review of lithium-ion battery state of charge estimation and management system in electric vehicle applications: challenges and recommendations, Renew. Sustain. Energy Rev. 78 (2017) 834–854, https://doi.org/10.1016/j.rser.2017.05.001.
[25] D.H. Doughty, C.C. Crafts, FreedomCAR Electrical Energy Storage System Abuse Test Manual for Electric and Hybrid Electric Vehicle Applications, Sandia Report, in: http://prod.sandia.gov/techlib/access-control.cgi/2005/053123.pdf, 2016, (Accessed 09 January 2019).
[26] A.G. Hsieh, S. Bhadra, B. Hertzberg, P.J. Gjeltema, A. Goy, J.W. Fleischer, D. Steingart, Electrochemical-acoustic time of flight: in operando correlation of physical dynamics with battery charge and health, Energy Environ. Sci. 8 (2015) 1569–1577, https://doi.org/10.1039/C5EE00111K.
[27] L. Gold, T. Bach, W. Virsik, A. Schmitt, J. Müller, T.E.M. Staab, G. Sextl, Probing lithium-ion batteries' state-of-charge using ultrasonic transmission – concept and laboratory testing, J. Power Sources 343 (2017) 536–544, https://doi.org/10.1016/j.jpowsour.2017.01.090.
[28] B. Sood, M. Osterman, M. Pecht, Health monitoring of lithium-ion batteries, Proc. 2013 IEEE Symp. Prod. Compliance Eng. (2013) 3–8, https://doi.org/10.1109/ISPCE.2013.6664165.
[29] G. Davies, K.W. Knehr, B. Van Tassell, T. Hodson, S. Biswas, A.G. Hsieh, D.A. Steingart, State of charge and state of health estimation using electrochemical acoustic time of flight analysis, J. Electrochem. Soc. 164 (12) (2017) A2746–A2755, https://doi.org/10.1149/2.1411712jes.
[30] C. Uhlmann, J. Illig, M. Ender, R. Schuster, E. Ivers-Tiffée, In situ detection of lithium metal plating on graphite in experimental cells, J. Power Sources 279 (2015) 428–438, https://doi.org/10.1016/j.jpowsour.2015.01.046.
[31] JM Energy, http://www.jmenergy.co.jp/en/product_whats.html (Accessed 09 January 2019).
[32] J.A. Jeevarajan, M.D. Martinez, Performance and safety of lithium-ion capacitors, Orlando, Florida; United States, Power Sources Conference; 46th; 9-12 Jun (2014).
[33] J. Ronsmans, B. Lalande, Combining energy with power: lithium-ion capacitors, Italy, International Symposium on Power Electronics, Electrical Drives, Automation and Motion (SPEEDAM 2016) (2016) 261–264 http://ieeexplore.ieee.org/stamp/stamp.jsp?tp=&arnumber=7525905.
[34] M. Arakawa, J. Yamaki, Anodic-oxidation of propylene carbonate and ethylene carbonate on graphite-electrodes, J. Power Sources 54 (1995) 250–254.

[35] J. Boltersdorf, S.A. Delp, J. Yan, B. Cao, J.P. Zheng, T.R. Jow, J.A. Read, Electrochemical performance of lithium-ion capacitors evaluated under high stress conditions for fast charge devices, Denver, Colorado, 48th Power Sources Conf. (2018) 296–299 http://www.powersourcesconference.com/PowerSources2018Digest/docs/17-4.pdf.

[36] M. Metzger, C. Marino, J. Sicklinger, D. Haering, Ha. Gasteiger, Anodic oxidation of conductive carbon and ethylene carbonate in high-voltage Li-ion batteries quantified by on-line electrochemical mass spectrometry, J. Electrochem. Soc. 162 (2015) A1123–A1134.

[37] S.A. Delp, O. Borodin, M. Olguin, C.G. Eisner, J.L. Allen, T.R. Jow, Importance of reduction and oxidation stability of high voltage electrolytes and additives, Electrochim. Acta209 (2016) 498–510.

[38] G.V. Zhuang, H. Yang, B. Blizanac, P.N. Ross, A study of electrochemical reduction of ethylene and propylene carbonate electrolytes on graphite using ATR-FTIR spectroscopy, Electrochem. Solid-State Lett. 8 (2005) A441.

[39] ASTM E1316-06, Standard Terminology for Nondestructive Examinations, ASTM International, West Conshohocken, PA, in: www.astm.org, 2006.

[40] B.P. Matadi, S. Geniès, A. Delaille, T. Waldmann, M. Kasper, M. Wohlfahrt-Mehrens, F. Aguesse, E. Bekaert, I. Jiménez-Gordon, L. Daniel, X. Fleury, M. Bardet, J.-F. Martin, Y. Bultel, Effects of biphenyl polymerization on lithium deposition in commercial graphite / NMC lithium-ion pouch-cells during calendar aging at high temperature, J. Electrochem. Soc. 164 (6) (2017) A1089–A1097, https://doi.org/10.1149/2.0631706jes.

[41] H. He, Y. Liu, Q. Liu, Z. Li, F. Xu, C. Dun, Y. Ren, M.X. Wang, J. Xie, Failure investigation of $LiFePO_4$ cells in over-discharge conditions, J. Electrochem. Soc. 160 (6) (2013) A793–A804, https://doi.org/10.1149/2.039306jes.

[42] M. Ouyang, D. Ren, L. Lu, J. Li, X. Feng, X. Han, G. Liu, Overcharge-induced capacity fading analysis for large format lithium-ion batteries with $LiyNi_{1/3}Co_{1/3}Mn_{1/3}O_2 + Li_yMn_2O_4$ composite cathode, J. Power Sources 279 (2015) 626–635, https://doi.org/10.1016/j.jpowsour.2015.01.051.